Int. J. Electrochem. Sci., 16 **(2021)** Article Number: 211051, doi: 10.20964/2021.10.06

International Journal of
ELECTROCHEMICAL
SCIENCE
www.electrochemsci.org

Short Communication

Stress Corrosion Cracking of 23Co14Ni12Cr3Mo Ultra-High Strength Steel in 3.5% NaCl Solution under Constant Load Condition

Chen Wen[1,2], *Junwei An*[1,*], *Liangxi Ding*[1], *Xiaolin Qiu*[1], *Shuhua Bai*[1]

[1] Nanchang Institute of Technology, Nanchang, Jiangxi, 311033, China;
[2] Beijing Spacecrafts, China Academy of Space Technology, Beijing, 100190, China
[*]E-mail: winstonewen@126.com

Received: 14 October 2020 / *Accepted:* 19 December 2020 / *Published:* 10 September 2021

The electrochemical responses including electrochemical impedance spectroscopy (EIS), potentiodynamic polarization (PP) and electrochemical noise (EN) in tress corrosion cracking (SCC) of 23Co14Ni12Cr3Mo ultra-high strength steel were investigated by using constant load (CL) tests. The fracture morphologies were characterized by scanning electron microscopy (SEM). The results showed that under the constant load, the SCC happens, and the reaction resistance of the sample decreases from 9602Ωcm^2 to 34.59Ωcm^2 with the time increases from 0h to 72h. And as the experiment time increases from 0h to 72h, the self-corrosion potential decreases from -0.426V to -0.626V, while the self-corrosion current increases from 7.02×10^{-6} A/cm^2 to 4.384×10^{-5} A/cm^2, which shows that as the reaction develops, the corrosion resistance of the sample decreases. Combined the EN response with fracture morphology, the SCC can be divided into three periods: The initial stage of corrosion initiation and development, the middle stage of stress corrosion expansion and the later transient period.

Keywords: 23Co14Ni12Cr3Mo, Potentiodynamic Polarization, Constant Load, Electrochemical Noise, Electrochemical Impedance Spectroscopy

1. INTRODUCTION

Stress corrosion cracking (SCC) of steels has been one of the threats to application in throughout the world [1~3]. As one of the most corrosive ions, chloride often induces stress corrosion to a sudden failure. Stress corrosion involves complex procedures such as electrochemical reaction and rust expansion. It is important to study the corrosion progress induced by chloride in the steel surface under stress.CL tests are often used to evaluate delayed fracture, stress corrosion cracking and unique corrosion[4~6]. Combined some proper characterization methods, the metal dissolution, applied stress [7], sensitizing temperature, sensitizing time, environmental factors [8,9] and HE[10] are investigated

by CL. Electrochemical measurements such as EIS and EN has been used to interpret the initiation and propagation progress of SCC under CL for a long period[11~14]. Diard [11,12] firstly used the impedance of electrochemical battery to study SCC and Bosch [13] distinguished between a flat electrode surface and an electrode surface with cracks by EIS methods. EN measurements were recently developed and applied to study the initiation and propagation of SCC under CL [14].

With excellent mechanical properties, the secondary hardening type of ultra-high strength steel 23Co14Ni12Cr3Mo is susceptible to SCC. Oehlert [15] studied the corrosion behavior of A100 steel with smooth tensile specimens by CL methods, which concluded that SCC could be occurred at constant stresses significantly below the 0.2% offset proof stress. Qian[16] found that the corrosion morphology was pitting corrosion, and gradually developed into uniform corrosion. Hu [17] investigated the HE properties of A100, and pointed out that coalition of micro-cracks accelerates the overall cracking process.

Previous studies on SCC of 23Co14Ni12Cr3Mo steel have concluded that the change of SCC susceptibility with strain rate can be divided into three regions [18-19]. In this work, the susceptibility of 23Co14Ni12Cr3Mo ultra-high strength steel to SCC was studied by using EIS and EN measurements under CL condition. The fracture surfaces were observed by SEM and the susceptibility to SCC was discussed.

2. EXPERIMENTAL

2.1 Material and heat treatment

The chemical composition of steel 23Co14Ni12Cr3Mo is shown in table 1, which was heat treated as follows: solution treated in vacuum at 885°C vacuum for 1h, air cooled to room temperature for 2h, chilled at -73°C for 1h, and tempered at 482 °C for 5h. The specimens for constant load tests were cut into the size shown in Fig.1.

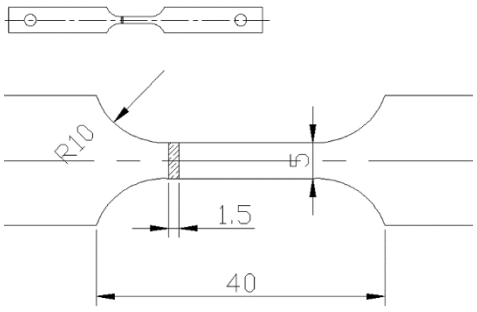

Figure1. Specimens for constant load test of 23Co14Ni12Cr3Mo

Table 1. Nominal composition of ultra-high strength steel 23Co14Ni12Cr3Mo,wt%

Material	C	Co	Ni	Cr	Mo	Fe
23Co14Ni12Cr3Mo	0.23	13.4	11.1	3.1	1.2	Bal.

2.2 Electrochemical measurements

The samples were loaded with a constant initial stress (80%σ_b), and the electrochemical noise tests were carried out until it broke. The constant load tests were carried out in 3.5 % wt NaCl solution at room temperature. The electrochemical measurements were performed by using a conventional three-electrode electrochemical cell on a Princeton 2273 electrochemical system with a 23Co14Ni12Cr3Mo of 1 cm in diameter as working electrode. A large platinum acted as the counter electrode. A saturated calomel electrode (SCE) was used and all potentials were referred to this electrode. All electrochemical experiments were performed in a 3.5 % wt NaCl solution at room temperature. The Open circuit potential (OCP) tests were carried out by potentiostat mode for 1800s. And the EIS was tested from 100kHz~10mHz, the dada was simulated by Zsimpwin software. The potentiodynamic polarization (PP) tests were scanned from -0.5V~0.5V(vs.ocp) at the rate of 5mV/s. The electrochemical noise (EN) tests were in-situ tested by three-electrode system under constant stress.

3. RESULTS AND DISCUSSION

3.1 OCP results

The ocp results of 23Co14Ni12Cr3Mo with different immersion time in 3.5% NaCl solution are shown in Fig1. As the immersion time increases from 0h to 72h, the open circuit potential gradually decreases from -0.34V to -0.54V, and the open circuit potential is very stable throughout the test, indicating that it has good corrosion resistance of 23Co14Ni12Cr3Mo steel.

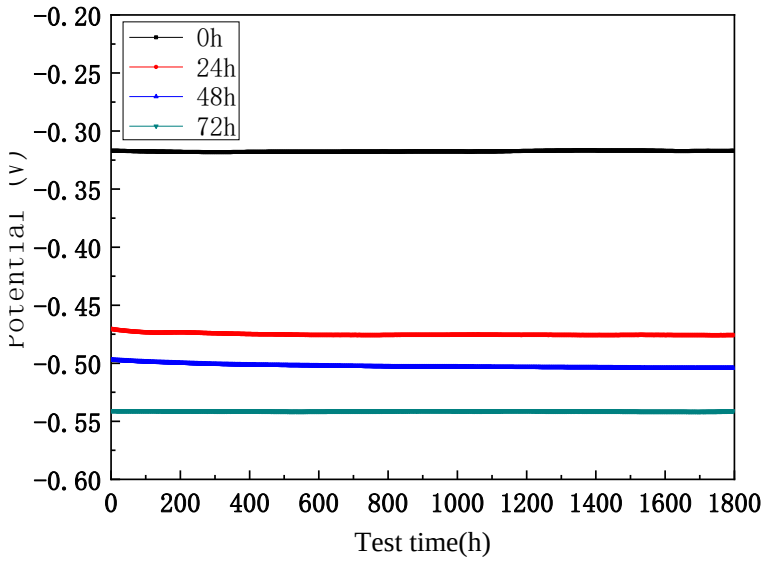

Figure 2. Open circuit potential curves after different immersion time in 3.5% NaCl solution of 23Co14Ni12Cr3Mo steel

3.2 EIS results

The electrochemical impedance spectroscopy (EIS) results and the fitting data by using the equivalent circuit model of Fig4 are given in Fig.3 and Table2, respectively. It can be seen that as the reaction time increases, the reaction resistance of the sample decreases from 9602Ωcm^2 to 34.59Ωcm^2. The specimen without immersion shows only one electric double layer structure, which indicates that the specimen for 0h has a good resistance. After immersion, the R_f and R_c are both decreases with the time increasing, which suggests that the corrosion resistance decreases in the NaCl solution.

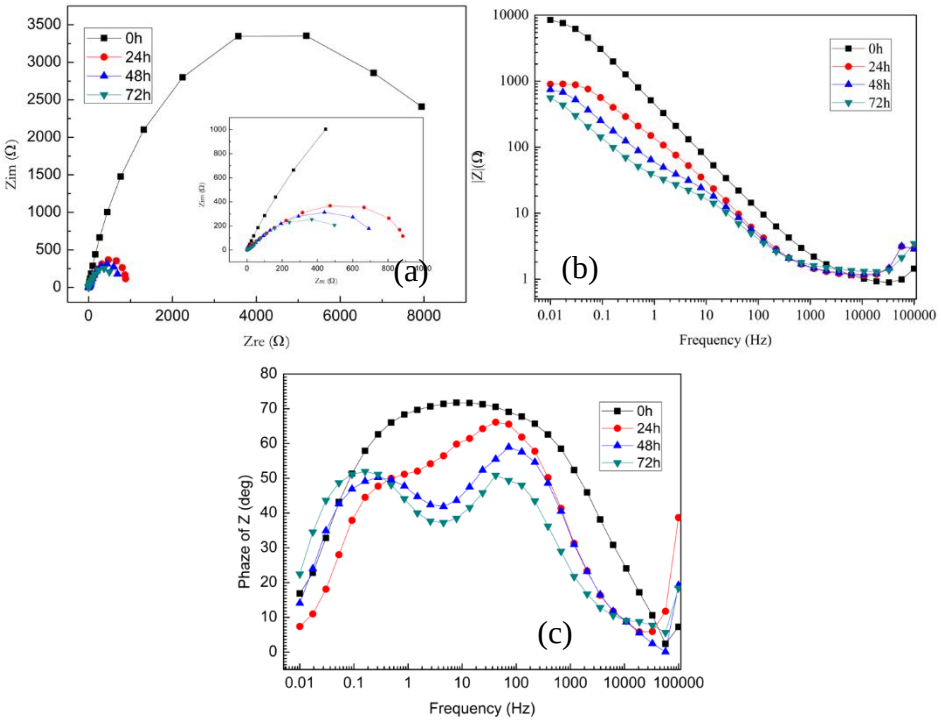

Figure 3. EIS analysis after different immersion time in 3.5% NaCl solution of 23Co14Ni12Cr3Mo steel.(a) Nyquist plots,(b) Bode plots, (c) Phase angle plots

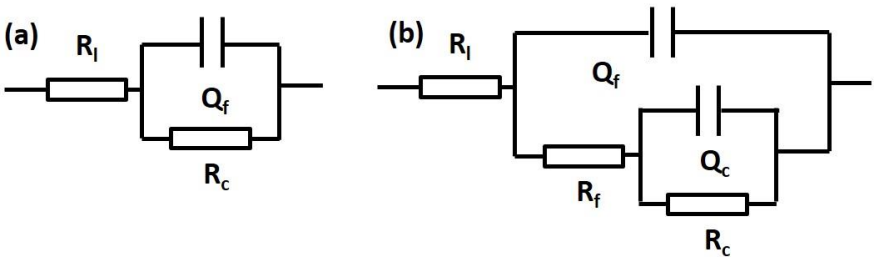

Figure 4. Equivalent circuit models of EIS (a:0h; b:24, 48, 72h) (R_l stands for solution resistance, Q_f and R_f are electric double layer capacitance and resistance respectively, Q_c and R_c are reaction capacitance and resistance respectively. Q is a constant phase angle element)

Table 2. The fitting results of EIS spectra by Zsimpwin software

Time	$R_l(\Omega cm^2)$	Q_f ($\Omega^{-1}s^n cm^2$)	n	$R_f(\Omega cm^2)$	Q_c ($\Omega^{-1}s^n cm^2$)	n	$R_c(\Omega cm^2)$
0h	0.8641	3.573×10^{-4}	0.799	--	--	--	9602
24h	1.086	7.897×10^{-4}	0.818	981.4	8.44×10^{-4}	0.8217	221.9
48h	1.113	1.178×10^{-3}	0.784	867	3.053×10^{-3}	0.784	51.96
72h	1.258	1.784×10^{-3}	0.752	722	8.266×10^{-3}	0.7893	34.59

3.3 EN results

The EN results with different immersion time in CL tests are shown in Fig 5. It can be seen that the electrochemical noise response can be divided into three stages. The pre-loading period (0-7200s) is the initiation and development reaction period. The current response amplitude gradually increases from 20mA/cm^2 to 40mA/cm^2. At the early stage of the reaction (0-500s), the current response cycle is longer, indicating that corrosion is gradually initiating; and with the extension of time, the current response cycle becomes shorter and the reaction intensifies. When the middle of the loading period, it is a stable expansion period (36000~128200s), and the current amplitude is small within 10 mA/cm^2, the load causes the sample to gradually deform, which is in the elastic strain process of the sample, promoting the further occurrence of electrochemical reactions. And the later period of loading is a rapid expansion period (172300-300000s), the sample gradually reaches into the plastic strain zone under constant load, the electrochemical reaction intensifies, and the sample achieves the instability process until it breaks.

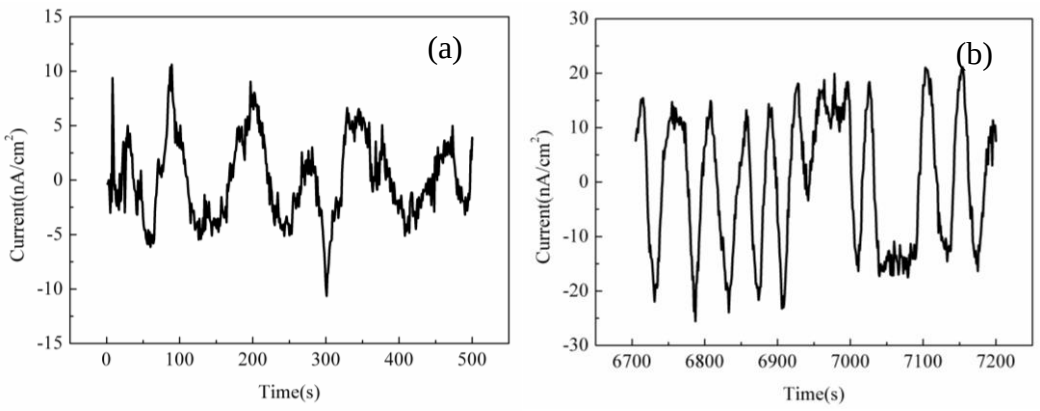

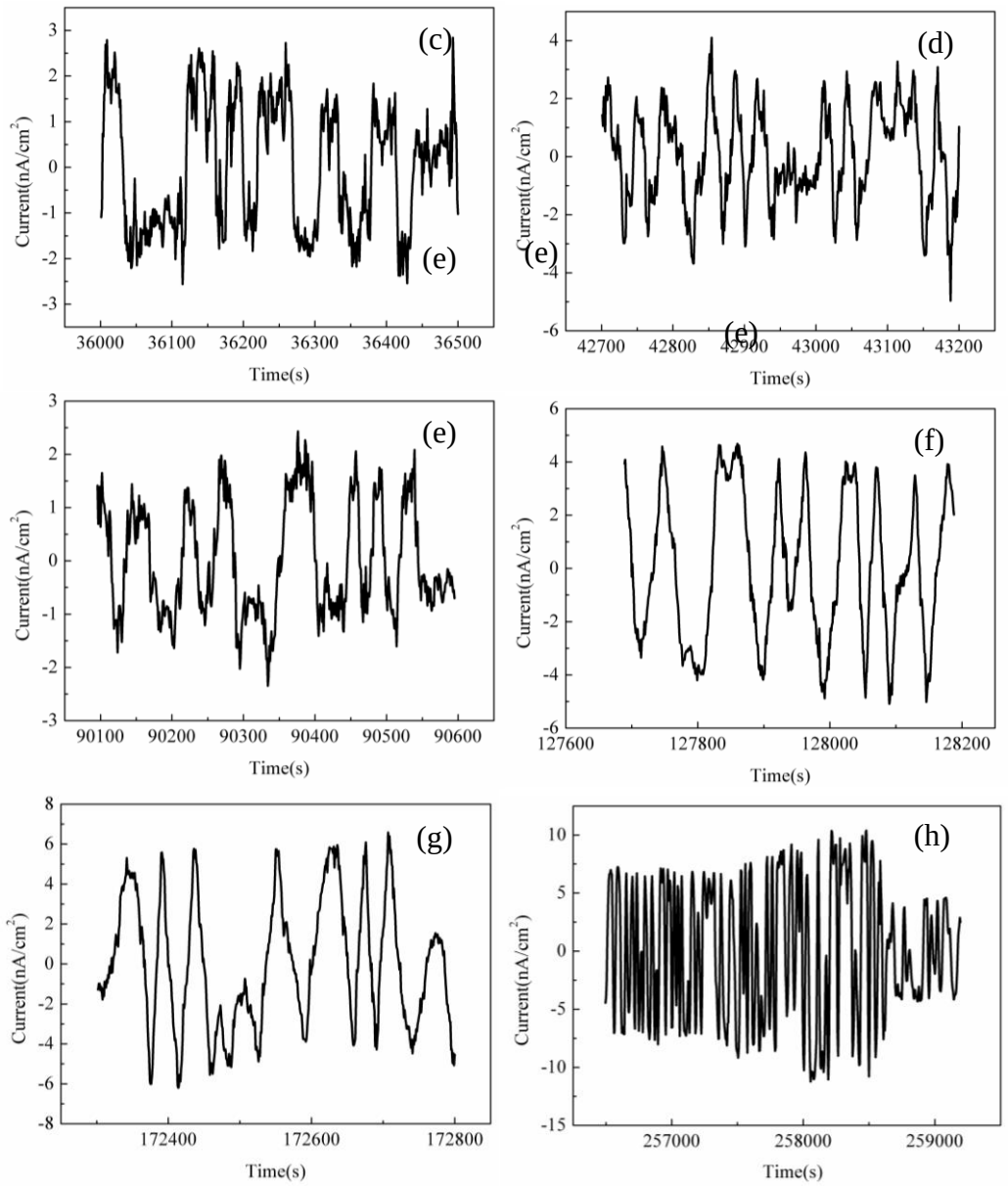

Figure 5. The electrochemical noise curves with loading time after 3.5% NaCl solution of 23Co14Ni12Cr3Mo steel. (a), 0-500s, (b) 6700-7200s, (c)36000-36500s, (d) 42700-43200s, (e) 90100-90600s, (f)127600-128200s, (g)172300-172800s, (h)256000-259000s

3.4 PP results

Fig.6 shows polarization curves of 23Co14Ni12Cr3Mo steel in 3.5% wt with different immersion time, and the fitted data is given in Table3. It can be seen that as the experiment time increases from 0h to 72h, the self-corrosion potential decreases from -0.426V to -0.626V, while the self-corrosion current increases from 7.02×10^{-6} A/cm^2 to 4.384×10^{-5} A/cm^2, which shows that as the reaction develops, the corrosion resistance of the sample decreases.

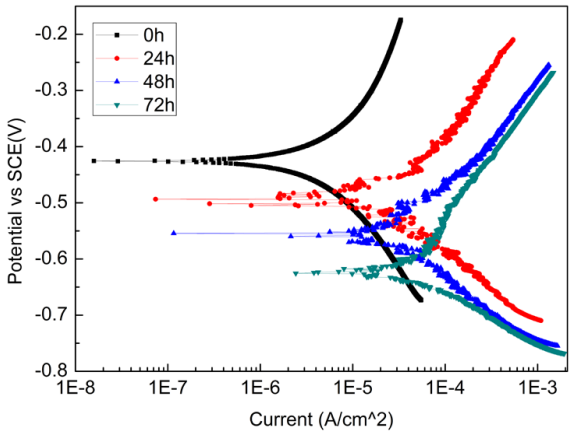

Figure 6. The potentiodynamic polarization curves after different immersion time in 3.5% NaCl solution of 23Co14Ni12Cr3Mo steel

Table 3. The fitted results of potentiodynamic polarization curves of 23Co14Ni12Cr3Mo steel

Time	Potential(V)	Current(A/cm^2)	R_a	R_c
0	-0.426	7.02×10^{-6}	0.04763	-0.499
24	-0.525	1.743×10^{-5}	0.0879	-0.1314
48	-0.554	2.002×10^{-5}	0.1137	-0.1256
72	-0.626	4.384×10^{-5}	0.2657	-0.8928

3.5 Fracture morphologies

The SEM morphology of the specimen is shown in Fig.7. From the macroscopic fracture morphology, it can be seen that the section can be divided into three areas, (I) crack initiation and surface corrosion area (A), the surface morphology is a lot of microcracks, covered by corrosion product; (II) stable expansion of plastic deformation area (B), this area is mainly an elongated dimple morphology, (III) a large area of transient region (C), the main morphology of this area is transgranular fracture, which is consistent with the electrochemical noise result.

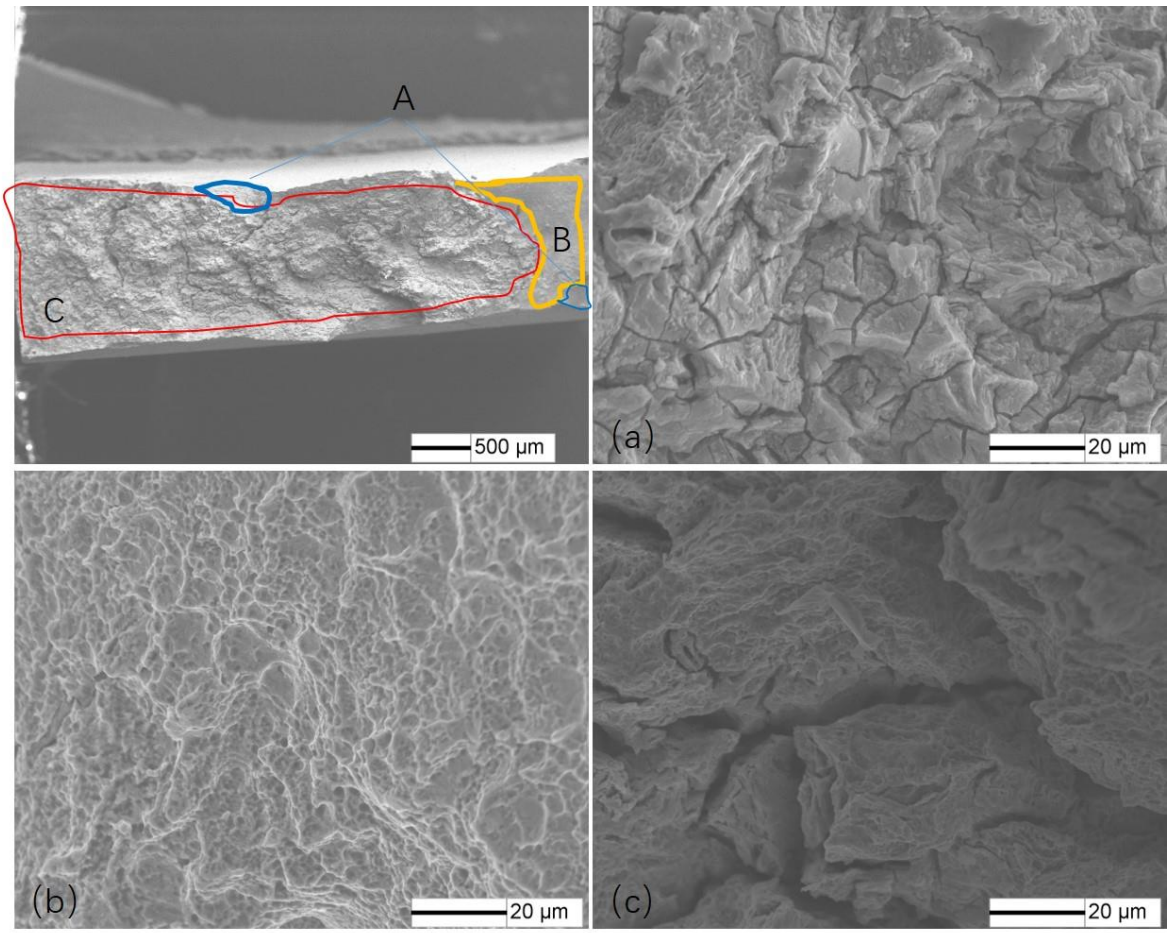

Figure 7. The fracture morphology of the specimen broken by constant load of 23Co14Ni12Cr3Mo steel (a), (b), (c) are micro morphology of zone A, B, C, respectively

3.6 Discussion

The electrochemical methods such as electrochemical noise signals, EIS, et al are detected in SCC reflecting the initiation and propagation of single micro cracks [22]. Analysis of the EN signals during SCC tests respect to time were useful in clearly demarcating SCC initiation stage from SCC propagation stages [23], which could be of much help in analyzing and judging the corrosion situation [24]. According to the electrochemical signals vs time, the SCC process can be divided into three periods under the constant load in NaCl solution. As chloride ions can penetrate the film, the corrosion initially on the outer surface [20-21]. The corrosion induced by chloride is a precursor to SCC, which is the initial period of SCC. The corrosion reduces the strength of 23Co14Ni12Cr3Mo steel and the load promotes corrosion, thus at the combined force of load and corrosion, the SCC happened though at the load of 80%σ_b, which can be found at the EN response and fracture morphology. That forms the second period of SCC. When the SCC further weakens the strength of the material, near or below the constant load, the sample breaks.

4. CONCLUSIONS

The SCC behavior of 23Co14Ni12Cr3Mo steel was studied with electrochemical and SEM methods, and it can be concluded as follows.

(1) Under the constant load, the SCC happens, and the reaction resistance of the sample decreases from 9602Ωcm^2 to 34.59Ωcm^2 with the time increases from 0h to 72h.

(2) As the experiment time increases from 0h to 72h, the self-corrosion potential decreases from -0.426V to -0.626V, while the self-corrosion current increases from 7.02×10^{-6} A/cm^2 to 4.384×10^{-5} A/cm^2, which shows that as the reaction develops, the corrosion resistance of the sample decreases.

(3) The SCC process can be divided into three periods: The initial stage of corrosion initiation and development, the middle stage of stress corrosion expansion and the later transient period, which can be found at the EN response and fracture morphology.

References

1. V. Giorgetti, E.A. Santos, J.B. Marcomini, V.L. Sordi. *Int. J. Pres Ves Pip.*, 169(2019)223.
2. H.K. Khan, N.Q. Zhang, W.Q. Xu, Z.L. Zhu, D.F. Jiang, H. Xu. *Int. J. Fatigue*., 118(2019)22.
3. S. Baragetti. E.V. Arcieri. *Int. J. Fatigue*, 112(2018)301.
4. L. Shen, W.C.D. Cheong, Y.L. Foo, Z. Chen. *Mater. Sci. Eng. A*. 532(2012)505.
5. H.S.D. Costa-Mattos, I.N. Bastos, J.A.C.P. Gomes. *Corros. Sci.*, 50(2008)2858.
6. R. Nishimura, J. Shirono, A. Jonokuchi. *Corros. Sci*., 50(2008) 2691.
7. R. Nishimura, Y. Maeda. *Corros. Sci*., 46(2004)755.
8. R. Nishimura. *Corros. Sci*., 49(2007)81.
9. K. Gao, D. Li, X. Pang, S. Yang. *Corros. Sci.*, 52(2010)3428.
10. E. Izumoto, R Nishimura. *Corros. Sci*., 53(2011)886.
11. J.P. Diard, B. Le Gorrec, C. Montella. *J. Power Sources*, 70(1998)78.
12. J.P. Diard, B. Le Gorrec, C. Montella, P. Landaud. *Electrochim. Acta*, 42(1997)3417.
13. R.W. Bosch. *Corros. Sci.,* 47(2005)125.
14. M. Breimesser, S. Ritter, H. P. Seifert, T. Suter, S. Virtanen. *Corros. Sci*., 63(2012)129.
15. A. Oehlert, A. Atrens. *Corros. Sci*., 38(1996)115.
16. J.H. Liu, S. Tian, S.M. Li, M. Yu. *Acta Aeron. Astron. Sinica*, 32(2011)1164.
17. A. Qian, P. Jin, X.M. Tan, D. Wang. *IOP Confer. Ser.: Mater. Sci. Eng.*, 394(2018)052066.
18. Y.B. Hu, C.F. Dong, H. Luo, K. Xiao, P. Zhong, X.G. Li. *Metall. Mater. Trans. A*., 48(2017)4046.
19. L.f. Wu, S.M. Li, J.H. Liu, M. Yu. *J. Centr. South Univ.*, 19(2012)2726.
20. N. Li, N. Ding, L. Liu, S.Q. Hu, S.Q.Sun, S. Qu, C.M.L. Wu. *J Fail. Anal. and Preven.*, 19(2019)29
21. L. Fan, Z.Y. Liu, W.M. Guo, J. Hou, C.W Du, X.G. Li. *Acta Metall. Sin.(Engl. Lett.)*, 28(2015) 866
22. M. Breimesser, S. Ritter, H.P. Seifert, T. Suter, S Virtanen. *Corros. Sci.* 63(2012)129.
23. G. Du, J. Li, W.K. Wang, C. Jiang, S.Z. Song. *Corros. Sci.* 53(2011)2918.
24. T. Anita, M.G. Pujar, H. Shaikh, R.K. DayaI, H.S. Khatak. *Corros. Sci.* 48(2006)2689.